

## MEMS Technologies and Devices for Single-Chip RF Front-Ends

Clark T.-C. Nguyen  
 Dept. of Electrical Engineering and Computer Science  
 University of Michigan  
 Ann Arbor, Michigan 48105-2122 USA  
 E-mail: [ctnguyen@umich.edu](mailto:ctnguyen@umich.edu)

### Abstract

*Micromechanical (or "μmechanical") components for communication applications fabricated via IC-compatible MEMS technologies and capable of low-loss filtering, mixing, switching, and frequency generation, are described with the intent to not only miniaturize and lower the parts counts of wireless front-ends via higher levels of integration, but also to eventually raise robustness (against interferers) and lower power consumption when used in alternative architectures that take advantage of the abundant frequency control enabled by RF MEMS devices. Among the devices described are vibrating micromechanical resonators with  $Q$ 's exceeding 10,000 at GHz frequencies; mechanical circuits comprised of such vibrating resonators; tunable MEMS-based capacitors and inductors with much higher  $Q$  than achievable by conventional IC counterparts; and RF MEMS switches with insertion losses and linearity superior to those attainable by present-day semiconductor switches.*

Keywords: single-chip, MEMS, micromechanical, quality factor, resonator, tunable capacitor, inductor, RF MEMS switch, filter, wireless communications, mechanical circuit

### 1.0 Introduction

Today's wireless transceivers are designed under a near mandate to minimize or eliminate, in as much as possible, the use of high- $Q$  passives. The reasons for this are quite simple: cost and size. Specifically, the ceramic filters, SAW filters, quartz crystals, and now FBAR filters, capable of achieving the  $Q$ 's from 500-10,000 needed for RF and IF bandpass filtering, and frequency generation functions, are all off-chip components that must interface with transistor functions at the board-level, taking up a sizable amount of the total board volume, and comprising a sizable fraction of the parts and assembly cost.

Pursuant to reducing the off-chip parts count in modern cellular handsets, direct-conversion receiver architectures [1] have removed the IF filter, and integrated inductor technologies are removing some of the off-chip  $L$ 's used for bias and matching networks [2]. Although these methods can lower cost, they often do so at the expense of increased transistor circuit complexity and more stringent requirements on

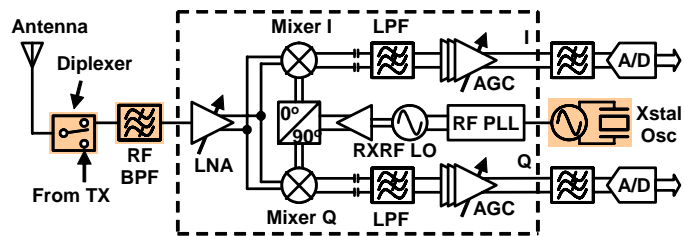


Fig. 1: System block diagram of a direct conversion wireless receiver front-end, showing the absence of an IF filter.

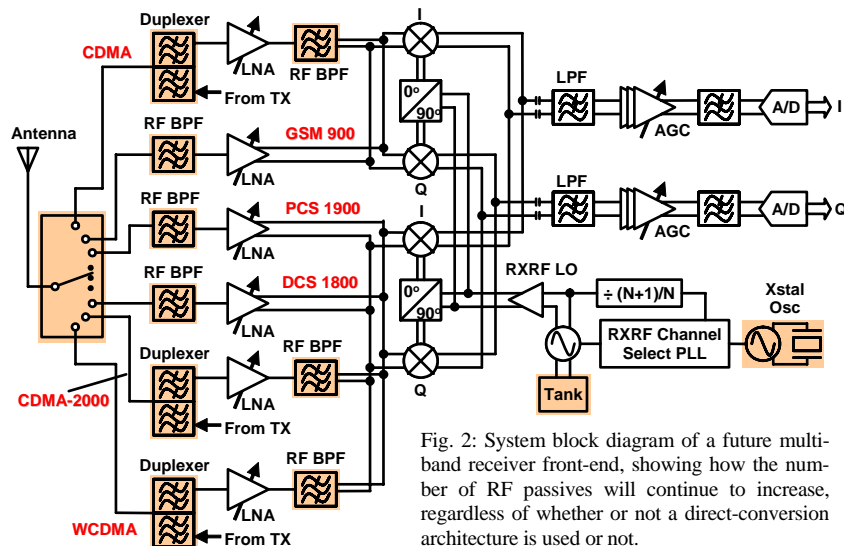


Fig. 2: System block diagram of a future multi-band receiver front-end, showing how the number of RF passives will continue to increase, regardless of whether or not a direct-conversion architecture is used or not.

circuit performance (e.g., dynamic range), both of which degrade somewhat the robustness and power efficiency of the overall system. In addition, the removal of the IF filter does little to appease the impending needs of future multi-band reconfigurable handsets that will likely require high- $Q$  RF filters in even larger quantities—perhaps one set for each wireless standard to be addressed. Fig. 1 and Fig. 2 compare the simplified system block diagram for a present-day handset receiver with one targeted for multi-band applications, clearly showing that it is the high- $Q$  RF filters, not the IF filter, that must be addressed. In the face of this need, and without a path by which the RF filters can be removed, an option to reinsert high  $Q$  components without the size and cost penalties of the past would be most welcome, especially if done in a manner that allows co-integration of passives with transistors onto the same chip.

Recent demonstrations of micro-scale high- $Q$  passive components that utilize microelectromechanical systems (MEMS) technology to allow on-chip integration alongside transistor circuits have sparked a resurgence of research interest in communication architectures that emphasize the use of high- $Q$  passive devices [3][4][5]. Among the most useful of these are vibrating micromechanical resonator circuits with  $Q$ 's greater than 10,000 at frequencies in the GHz range [6][7][8]; tunable  $\mu$ mechanical capacitors with  $Q$ 's up to 300 at 1 GHz [9][10];  $\mu$ machined inductors with  $Q$ 's up to 85 at 1 GHz [11]; and  $\mu$ mechanical switches with insertion losses as low as 0.1dB [12]—all achieved in orders of magnitude smaller size than macroscopic counterparts, and with little or no power consumption. Much of the interest in these “RF MEMS” devices originally derived from their amenability to on-chip integration alongside transistors, which might someday enable a single-chip RF front-end that includes both transistors and high- $Q$  passives.

But even if only the high- $Q$  passives shaded in Fig. 2 are integrated onto a single-chip (c.f., Fig. 3), and not integrated together with transistors but rather combined as perhaps two chips, the cost and size savings would still be quite substantial. In particular, if the on-chip passives technology is such that device properties (e.g., frequencies) can be specified by CAD-definable quantities (e.g., *lateral* dimensions, as opposed to thickness), allowing them to be defined in a single deposited layer, then the cost of a single chip of *all* 11 of the high- $Q$  passives in Fig. 2 could potentially end up being about the same as *one* of the original off-chip passives. Needless to say, this degree of cost reduction creates great incentive for development of lateral vibration-mode MEMS resonators, for which frequency is defined by CAD-definable *lateral* dimensions; as opposed to thickness

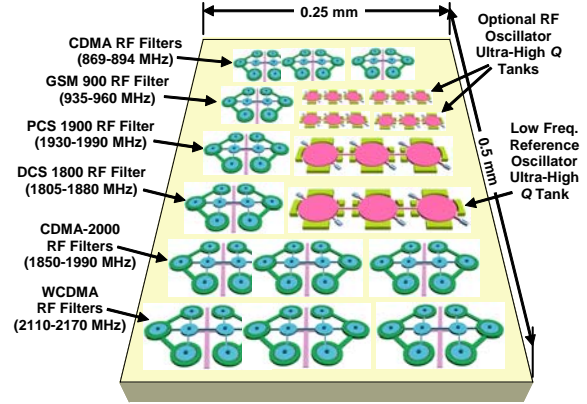


Fig. 3: Schematic of a single-chip of high- $Q$  passives made possible by lateral-mode vibrating MEMS resonator technology. Here, a resonator technology that allows many different frequencies to be defined (e.g., via CAD layout) in a single film layer is assumed. The above  $0.25 \times 0.5 \text{ mm}^2$  chip includes the receive path high- $Q$  passives of Fig. 2, plus additional oscillator tanks for improved phase noise and injection locking suppression. Although only receive path high- $Q$  filters are included, here, note that transmit filters, as well as other lateral-dimension-defined passives described in this paper, could also be added while still retaining a tiny chip size.

mode resonators (e.g., FBAR's or shear-mode quartz) that require a different film thickness for each individual frequency, and thus, impose higher cost. If the lateral-mode resonators use capacitive transduction, then they possess the additional advantage of self-switchability [13], which allows the system of Fig. 2 to dispense with the multi-throw switch, and hence, dispense with its size, cost, and series insertion loss.

From a broader perspective, size reduction aside, it is actually the potential of on-chip micromechanical high- $Q$  passives to enhance robustness and reduce power consumption in alternative transceiver architectures that makes them so compelling. In particular, the availability of high- $Q$  on-chip passives might eventually enable a paradigm-shift in transceiver design where the advantages of high- $Q$  (e.g., in filters and oscillators) are emphasized, rather than suppressed [3][5]. For example, like transistors, micro-mechanical elements can be used in large quantities without adding significant cost. This not only brings more robust superheterodyne architectures back into contention, but also encourages modifications to take advantage of a new abundance in low loss ultra-high- $Q$  frequency shaping at GHz frequencies. For example, an RF channel-select filter bank may now be possible, capable of eliminating not only out-of-band interferers, but also out-of-channel interferers, and in so doing, relaxing the dynamic range requirements of the LNA and mixer, and the phase noise requirements of the local oscillator, to the point of perhaps allowing complete transceiver implementations using very low cost transistor circuits (e.g., perhaps eventually even organic circuits).

After very briefly describing fundamental charac-

teristics behind the MEMS technologies that make them possible, this paper presents an overview of the RF MEMS devices expected to play key roles in realizing the above paradigm-shift in wireless transceiver implementation.

## 2.0 MEMS Technology

The majority of RF MEMS devices most useful for communications applications are based on tiny micromechanical structures suspended above the substrate. There are now a wide array of MEMS technologies capable of attaining such on-chip micro-scale suspended mechanical structures, each distinguishable by not only the type of starting or structural material used (e.g., silicon, silicon carbide, metals, glass, plastic, etc.), but also by the method of micromachining (e.g., surface, bulk, 3D growth, etc.), and by the application space (e.g., optical MEMS, bio MEMS, etc.). For the present focus on portable communications, MEMS technologies amenable to low capacitance merging of micromechanical structures together with integrated transistor circuits are of most interest. In this regard, surface micromachining technologies, where structural materials are obtained exclusively via deposition or plating processes, are among the most applicable to the present discussion.

Fig. 4 presents key cross-sections describing a polysilicon surface micromachining process done directly over silicon CMOS circuits. As shown, this process entails depositing and patterning films above the CMOS circuits using the same equipments already found in CMOS foundries until a cross section as in Fig. 4(a) is achieved. Here, the structural polysilicon layer has been temporarily supported by a sacrificial oxide film during its own deposition and patterning. After achieving the cross-section of Fig. 4(a), the whole wafer is dipped into an isotropic etchant, in this case hydrofluoric acid, which attacks only the oxide sacrificial layer, removing it and leaving the structural polysilicon layer intact, free to move in multiple dimensions. Fig. 5 presents the SEM of a watch oscillator that combines a 16 kHz folded-beam micromechanical resonator with sustaining CMOS transistor circuits using this very process flow, but with tungsten as the metal interconnect in order to accommodate  $625^\circ$  structural polysilicon deposition temperatures [14].

The process of Fig. 4 features a high degree of modularity, where the MEMS and transistor processes are not intermixed, but rather combined in separate modules, one for the transistors, one for the MEMS. A modular merging process is in principal much preferred over one that mixes process steps from its constituent technologies, since it can adapt more easily to advances in each individual module; whereas an intermixed process would likely need to

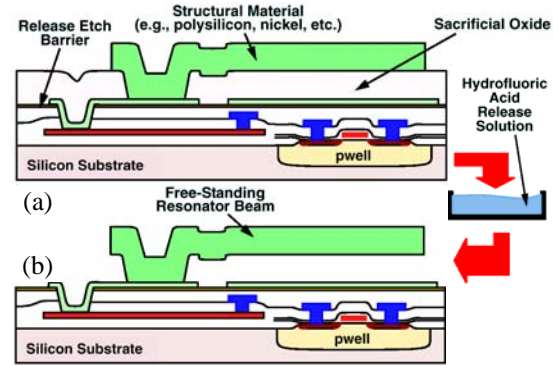


Fig. 4: Cross-sections (a) immediately before and (b) after release of a surface- $\mu$ machining process done directly over CMOS [14].

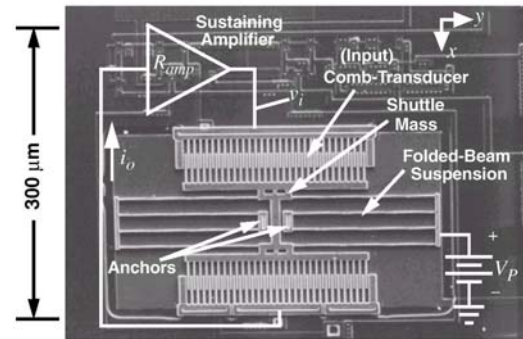


Fig. 5: SEM of a fully integrated 16-kHz watch oscillator that combines CMOS and MEMS in a single fully planar process [14].

be redesigned from scratch to accommodate advances in either of the merged processes. Despite this advantage, MEMS/transistor merging processes based on intermixing of steps still dominate the high volume MEMS accelerometer market [15], mainly because so far, no modular technology has been truly modular. For example, the process of Fig. 4 falls short of perfect modularity in its use of tungsten as the interconnect metal, which represents a deviation from the standards of the mainstream IC industry, which has already directed enormous resources towards multi-level interconnects in aluminum, and more recently, copper metallization. Given the very low probability that the IC industry would adapt tungsten metallization just to accommodate MEMS devices, research to lower the temperature required for the structural material deposition and annealing is presently underway. Among the top material candidates are SiGe [16], amorphous silicon [17], and CVD polydiamond [6].

## 3.0 Micromechanical RF Devices

Table 1 through Table 4 summarize the RF MEMS devices most useful for communications applications. These devices are now described.

### 3.1 High- $Q$ Vibrating Micromechanical Resonators

Because mechanical resonances generally exhibit



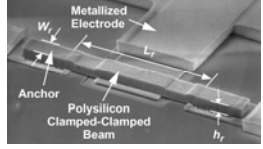
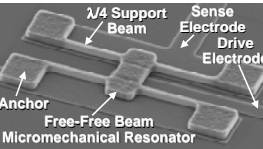
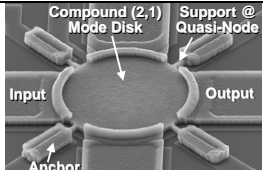
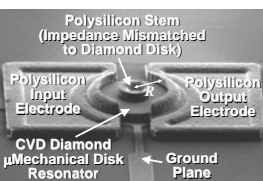
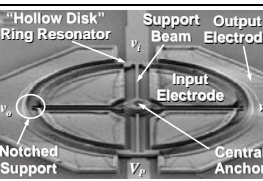
orders of magnitude higher  $Q$  than their electrical counterparts, off-chip vibrating mechanical resonators (e.g., quartz crystals, SAW resonators) capable of achieving  $Q$ 's  $>1,000$  are already essential components in communication circuits. With appropriate scaling via MEMS technology, such devices can not only be integrated alongside transistors on a single-chip, but can also be designed to vibrate over a very wide frequency range, from 1 kHz to  $>1$  GHz, making them ideal for ultra stable oscillator and low loss filter functions at common transceiver frequencies. On this point, as already mentioned in Section 1.0, resonator types that allow specification of frequency via CAD-definable parameters (e.g., *lateral*, rather than thickness, dimensions) are most attractive, since they allow realization of many different frequencies in a single layer.

### 3.1-1 Capacitively Transduced Micromechanical Resonators

Among lateral-mode micromechanical resonators, capacitively transduced ones so far exhibit the highest frequency- $Q$  products, since they generally are constructed in single high quality materials, and thus suffer less from the material interface losses that can encumber other transducer types (e.g., piezoelectric). In addition to better  $Q$ , capacitive transduction also offers more flexible geometries with CAD-definable frequencies, voltage-controlled reconfigurability [13][18], better thermal stability [19], material compatibility with integrated transistor circuits, and an on/off self-switching capability [13], all of which contribute to a strong amenability to mechanical circuit design.

Table 1 succinctly presents the evolution of capacitively transduced vibrating  $\mu$ mechanical resonator geometries over the past ten years. As shown, clamped-clamped beam resonators (row 1 of Table 1), which are essentially guitar strings scaled down to  $\mu\text{m}$  dimensions to achieve VHF frequencies, can achieve on-chip  $Q$ 's  $\sim 8,000$  for oscillator and filtering functions in the HF range. However, anchor losses in this specific structure begin to limit the achievable  $Q$  at higher VHF frequencies, limiting the practical range of this structure to  $<100$  MHz when using  $\mu\text{m}$ -scale dimensions. To achieve higher frequency while retaining  $Q$ 's in the thousands and without the need for sub- $\mu\text{m}$  dimensions [23] (which can potentially degrade the power handling and fre-

**Table 1: High Frequency- $Q$  Product Vibrating RF MEMS Devices**

	Photo	Performance
CC-Beam Resonator [20]		Demo'ed: $Q \sim 8,000$ @ 10 MHz (vac) $Q \sim 50$ @ 10 MHz (air) $Q \sim 300$ @ 70 MHz (anchor diss.) $Q$ drop w/ freq. limits freq. range Series Resistance, $R_x \sim 5\text{-}5,000\Omega$
FF-Beam Resonator [21]		Demo: $Q \sim 28,000$ @ 10-200 MHz (vac) $Q \sim 2,000$ @ 90 MHz (air) No drop in $Q$ with freq. Freq. Range: $>1\text{GHz}$ ; unlimited w/ scaling and use of higher modes Series Resistance, $R_x \sim 5\text{-}5,000\Omega$
Wine-Glass Disk Res. [22]		Demo'ed: $Q \sim 156,000$ @ 60 MHz (vac) $Q \sim 8,000$ @ 98 MHz (air) Perimeter support design nulls anchor loss to allow extremely high $Q$ Freq. Range: $>1\text{GHz}$ w/ scaling Series Resistance, $R_x \sim 5\text{-}5,000\Omega$
Contour-Mode Disk Res. [6][8]		Demo'ed: $Q \sim 11,555$ @ 1.5 GHz (vac) $Q \sim 10,100$ @ 1.5 GHz (air) Balanced design and material mismatching anchor-disk design nulls anchor loss Freq. Range: $>1\text{GHz}$ ; unlimited w/ scaling and use of higher modes Series Resistance, $R_x \sim 50\text{-}50,000\Omega$
Hollow Disk Ring Res. [7]		Demo'ed: $Q \sim 15,248$ @ 1.46 GHz (vac) $Q \sim 10,165$ @ 1.464 GHz (air) $\lambda/4$ notched support nulls anchor loss Freq. Range: $>1\text{GHz}$ ; unlimited w/ scaling and use of higher modes Series Resistance, $R_x \sim 50\text{-}5,000\Omega$

quency stability of these devices in present-day applications [24]), more balanced structures that eliminate anchor losses can be used, such as the free-free beam [21] in row 2; the wine-glass [22] and contour-mode disks [6][8] in rows 3 and 4; and the ring [7] in row 5 of Table 1. The disks and ring of this group already operate beyond GHz frequencies with  $Q$ 's greater than 10,000 (in both vacuum and air), all while retaining sufficiently large dimensions to maintain adequate power handling and to avoid "scaling-induced" phenomena, such as mass-loading or temperature fluctuation noise [24], that might degrade performance when dimensions become too small.

The device of row 4 of Table 1 consists of a 20 $\mu\text{m}$ -diameter, 2 $\mu\text{m}$ -thick polydiamond disk suspended by a polysilicon stem self-aligned to be exactly at its center, all enclosed by polysilicon electrodes spaced 80 nm from the disk perimeter. When vibrating in its radial contour mode, the disk expands and contracts around its perimeter in what effectively amounts to a high stiffness, high energy, extensional mode. Since the center of the disk corresponds to a node location for the radial contour vibration mode shape, anchor losses through the supporting stem are

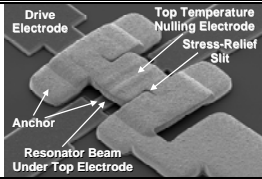
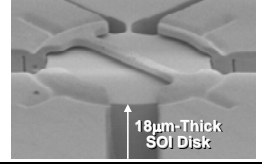
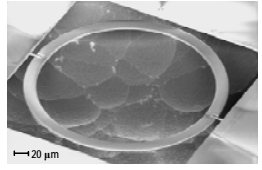
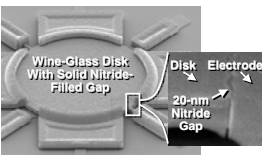
greatly suppressed, allowing this design to retain a very high  $Q$  even at this UHF frequency. In addition to the GHz data shown in row 4 of Table 1, a version of this device at 498 MHz achieves a  $Q$  of 55,300 in vacuum [6], which corresponds to a frequency- $Q$  product of  $2.75 \times 10^{13}$ —the highest for any resonator in the GHz range at room temperature. Furthermore, the high stiffness of its radial contour mode gives this resonator a much larger total (kinetic) energy during vibration than exhibited by previous resonators, making it less susceptible to energy losses arising from viscous gas damping, hence, allowing it to retain  $Q$ 's  $>10,000$  even at atmospheric pressure. This resonator not only achieves a frequency applicable to the RF front ends of many commercial wireless devices, it also removes the requirement for vacuum to achieve high  $Q$ , which should greatly lower the cost of this technology.

It should be noted that the disk of row 4 in Table 1 is constructed of polydiamond, which has twice the acoustic velocity of polysilicon, so facilitates the realization of GHz frequency. However, polysilicon structural material can also achieve similar performance when designed with the right geometry and isolating anchoring, as exemplified by the ring resonator of row 5 in Table 1, which uses a centrally located quarter-wavelength support structure with ring notches to minimize anchor losses towards  $Q$ 's  $>10,000$  in both vacuum and air at 1.46 GHz.

### 3.1-2 Thermal Stability, Aging, and Impedance

Besides frequency range and  $Q$ , thermal stability, aging/drift stability, and impedance, are also of utmost importance. Table 2 presents some of the  $\mu$ mechanical resonator devices designed specifically to address these parameters. In particular, the beam device of row 1 in Table 2 utilizes a temperature-tailored top electrode-to-resonator gap spacing to attain a total frequency deviation over 25-125°C of only 18 ppm, which actually betters that of AT quartz. This, combined with recent demonstrations of good aging and drift [27][28], makes  $\mu$ mechanical resonators excellent candidates for reference oscillator applications in communication circuits. In addition, the devices of rows 2 and 3 illustrate strategies for lowering the impedances of stand-alone resonators, the first based on enlargement of the electrode-to-resonator capacitive overlap area to increase electromechanical coupling [25]; the second dispensing with capacitive transducers, and using piezoelectric transducers [26][30]; with the latter so far being the more successful in achieving the 50-377 $\Omega$  imped-

**Table 2. Thermal Stability and Impedance of Microresonators**

	Photo	Performance
Electrical Stiff. Comp. Res. [19]		Demo'ed: $Q \sim 4,000$ @ 10MHz (vac) Temperature-tailored gap to effect an electrical stiffness variation that cancels Young's modulus variation 18 ppm freq. variation over 27-107°C
SOI Silicon WG-Disk [25]		WGDisk: $Q \sim 26,000$ @ 149MHz (air) SiBAR: $Q \sim 40,000$ @ 137 MHz (vac) $Q \sim 3,700$ @ 983 MHz SOI thickness to effect large capacitive overlap for low Series Resistance, $R_x \sim 5.5k\Omega$ @ 137 MHz
Lateral Piezoelec. Ring [26]		Demo'ed: $Q \sim 2,900$ @ 473 MHz (air) Contour-mode ring-shaped AlN piezoelectric resonator Driven laterally via the $d_{31}$ coeff., so freqs. determined by lateral dims. Series Resistance, $R_x \sim 80\Omega$
Solid-Gap Disk Resonator [29]		Demo'ed: $Q \sim 25,300$ @ 61MHz (vac) Solid nitride-filled electrode-to-resonator gap (20 nm) Much better yield and able to achieve low impedance at low dc-bias voltage Series Resistance, $R_x \sim 1.5k\Omega$ @ 4V

ances desired for matching to off-chip components.

Although it does achieve low impedance, and is amenable to CAD specification, the piezoelectric device of row 3 in Table 2 still sacrifices the important high  $Q$ , on/off self-switching, and temperature stability attributes offered by capacitive transducers. To attain impedances similar to that of the row 3 device, yet retain capacitive transduction and all of its benefits, the device of row 4 has very recently been introduced. This 61-MHz wine-glass mode device is identical in shape and operation to that of row 3 in Table 1, but is now equipped with a solid dielectric-filled capacitive transducer gap (to replace the previous air gap) that reduces its impedance by  $8\times$  over its air-gap counterpart, while allowing it to retain a very high  $Q$  of 25,300 [29]. In addition to lower motional resistance, the use of solid dielectric-filled transducer gaps provides numerous other practical advantages over the air gap variety, since it (1) better stabilizes the resonator structure against shock and microphonics; (2) eliminates the possibility of particles getting into an electrode-to-resonator air gap, which poses a potential reliability issue; (3) greatly improves fabrication yield, by eliminating the difficult sacrificial release step needed for air gap devices; and (4) potentially allows larger micromechanical circuits (e.g., bandpass filters comprised of interlinked resonators) by stabilizing constituent resonators as the circuits they comprise grow in complexity.

### 3.1-3 Vibrating

#### Micromechanical Circuits

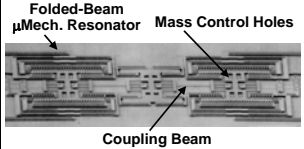
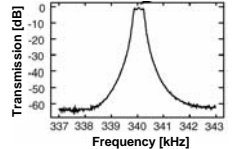
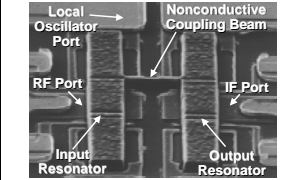
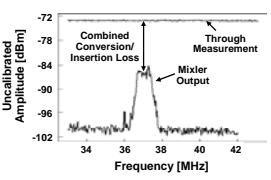
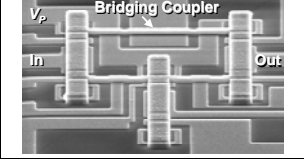
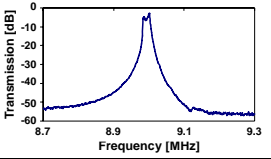
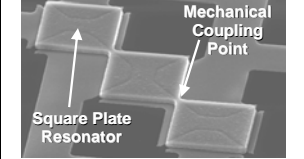
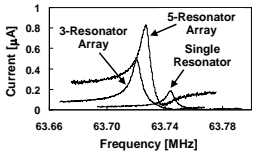
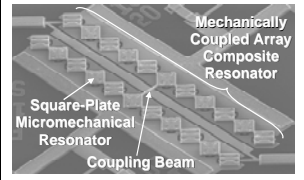
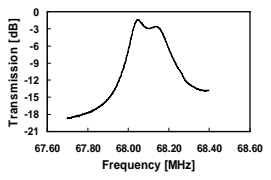
Although stand-alone vibrating  $\mu$ mechanical resonators are themselves quite applicable to local oscillator synthesizer applications in transceivers, their application range can be greatly extended by using them in circuit networks. To date, the simplicity and circuit amenability of capacitive transducers has allowed them to realize the most complex on-chip purely mechanical circuits.

Table 3 summarizes several purely micromechanical circuits, from bandpass filters with impressive on-chip insertion losses of only 0.6dB for 0.09% bandwidth [31], some using non-adjacent bridging to effect loss poles [32]; to mixer-filter (“mixer”) devices that both translate and filter frequencies via a single passive structure [18]; to impedance transforming mechanically-coupled arrays that combine the responses of multiple high-impedance resonators to allow matching to a much lower  $50\Omega$  [33]; to a filter using mechanically-coupled composite resonators to allow matching to  $50\Omega$  while attaining the lowest insertion loss to date for a VHF on-chip micromechanical filter [34].

Each of the filters in Table 3 are comprised of several identical resonator elements coupled by mechanical links attached at very specific locations on the resonators. As detailed more fully in [20] and [31], the center frequency of such a mechanical filter is determined primarily by the (identical) frequencies of its constituent resonators, while the spacings between modes (i.e., the bandwidth) is determined largely by a ratio of the stiffnesses of its coupling beams to that of the resonators they couple at their attachment locations. The circuit nature of each filter in Table 3 is emphasized by the fact that each was designed using equivalent electrical circuits defined by electromechanical analogies [20][31], which allowed the use of electrical circuit simulators, like SPICE—an important point that implies mechanical circuits should be amenable to the vast automated circuit design environments already in existence.

The arraying used in the devices of rows 4 and 5 not only provides a lower filter termination imped-

Table 3: Summary of Vibrating Micromechanical Circuits

	Photo	Data	Performance
3-Res. Folded-Beam Filter [31]			Freq. = 340 kHz BW = 403 Hz %BW = 0.09% StopB Rej. = 64 dB Ins. Loss < 0.6 dB
Mixer-Filter [18]			Mixes a 240MHz RF down to 37MHz IF, then filters Conv. Loss = 9.5dB %BW = 1.7% Ins. Loss = 3.5dB
3 Res. Bridged CC-Beam [32]			Freq. = 9 MHz BW = 20 kHz %BW = 0.2% StopB Rej. = 51 dB Ins. Loss < 2.8 dB
Mech.-Coupled Res. Array [33]			Automatic matching of resonators achieved via mech. coupling; current multiplied by number of resonators $N$
Array Composite Filter [34]			Freq. = 68.1 MHz BW = 190 kHz %BW = 0.28% StopB Rej. = 25 dB Ins. Loss < 2.7 dB

ance by increasing the effective capacitive transducer overlap area, but also raises the 3<sup>rd</sup> order intermodulation intercept point ( $IP_3$ ) of the composite device [35][36] (i.e., raises its linearity) in the process. The use of an array of resonators to match the impedance of a micromechanical circuit to an off-chip macroscopic element (e.g., an antenna) is really no different from the use of a cascade of progressively larger inverters (in layout, arrays of smaller inverters) to allow a minimum-sized digital gate to drive an off-chip board capacitor. In essence, micro (or nano) scale circuits, whether they be electrical or mechanical, prefer to operate with higher impedances than macro-scale ones, and interfacing one with the other requires a proper impedance transformation. In a building block circuit environment, such an impedance transformation is most conveniently accomplished via large numbers of circuit elements, whether they be electronic transistors or mechanical resonators.

Table 3 also implicitly indicates the progression of micromechanical circuit complexity with time. In particular, the composite array filter in row 5 uses more than 43 resonators and links, which qualifies it as a medium-scale integrated (MSI) micromechanical



circuit. And this is just the beginning. After all, the aforementioned RF channel-select filter banks [3][5] aim to use hundreds or thousands of filters like this, which would inevitably lead to LSI or VLSI micromechanical circuits. When combined (preferably on the same chip [14][15][16]) with transistor integrated circuits, the time domain prowess of transistors can be merged with the frequency domain capabilities of mechanical circuits to achieve even greater functionality.

### 3.2 Medium- $Q$ Passives

In addition to devices with  $Q$ 's  $>1,000$ , medium- $Q$  passives with  $Q$ 's from 20-100 are also often used in communication circuits for biasing and impedance matching purposes, as well as for VCO frequency-setting tanks and coarse front-end frequency selection. Although the pn diodes and planar spiral inductors of *conventional* IC technology can achieve  $Q$ 's  $\sim 7$  suitable for bias and matching networks, process modifications, such as the MEMS-enabled ones summarized in Table 4, are needed to attain  $Q$ 's  $>20$ .

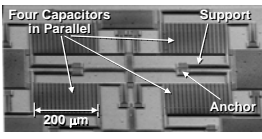
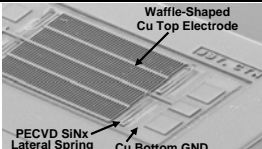
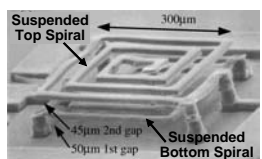
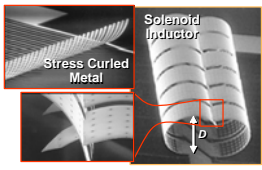
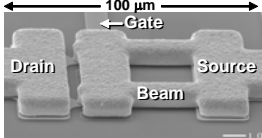
#### 3.2-1 High- $Q$ Tunable Capacitors

Tunable  $\mu$ mechanical capacitors, summarized in rows 1 and 2 of Table 4, consist of metal plates that can be moved with respect to one another, often via electrostatic means, allowing voltage-control of the capacitance between the two plates. Because low-resistance metal materials can be used in their construction,  $Q$ 's as high as 300 can be attained [10]—much higher than attainable by lossy semiconductor pn diodes offered by conventional IC technology. Paired with medium- $Q$  inductors,  $\mu$ mechanical capacitors can enhance the performance of low noise VCO's. In addition, if inductors could be achieved with  $Q$ 's as high as 300, tunable RF pre-select filters might be attainable that could greatly simplify the implementation of multi-band transceivers.

#### 3.2-2 Medium- $Q$ Micromachined Inductors

As mentioned above, tunable  $\mu$ mechanical capacitors must be paired with inductors with  $Q > 20$  to maximize their utility in communication circuits. Unfortunately, due to excessive series resistance and substrate losses, conventional IC technology can only provide spiral inductors with  $Q$ 's no higher than  $\sim 7$  [2]. Even slightly modified IC technologies that attempt to curtail substrate eddy current losses by raising the substrate resistance (e.g., by damaging the substrate surface [40]) or opening slots in metal ground planes [2] have not been able to raise  $Q$ 's to

**Table 4. Medium- $Q$  Passives and RF MEMS Switches**

	Photo	Performance
Tunable Plate Capacitor [9]		Demo'ed: $Q \sim 60$ @ 1GHz for 2.2pF Contact & interconnect $R$ limit $Q$ Capacitance: 1-4pF Tuning range $\sim 16\%$ over 5.5V Successfully used in low noise VCO
Mov. Dielectric Capacitor [10]		Demo'ed: $Q \sim 300$ @ 1GHz for 1.2 pF Movable dielectric mechanism for $\Delta C$ allows lower contact/interconnect $R$ Self-resonance $\sim 19$ GHz Tuning range $\sim 7.7\%$ over 10V
Suspended Spiral Inductor [37][38]		Demo'ed: $Q \sim 28$ @ 1.8GHz for 5nH $W_{wind}=30\mu\text{m}$ , $h_{wind}=15\mu\text{m}$ , $L \sim 1.4\text{nH}$ using suspended, thick copper Two spirals allows use of mutual $L$ to avoid substrate eddy currents 1 spiral: $Q \sim 70$ @ 6GHz for 1.38nH
Self-Assembled Solenoid [11]		Demo'ed: $Q \sim 85$ @ 1GHz for 7.5nH 5 turns $\Rightarrow$ self-resonance of 2.7GHz Stress-curved interlocked solenoid turns w/ $B$ fields parallel to low $R$ substrate that reduces eddy currents
$\mu$ Mechanical Switch [39]		Demo'ed: Packaged Ins. Loss $< 0.35\text{dB}$ @ 10GHz, $< 0.45\text{dB}$ @ 35GHz $>600$ billion cycles cold switched Other (packaged) switches: $< 0.2\text{dB}$ loss @ Ka-band (but less lifetime)

the 20's for needed inductance values at the low GHz wireless radio frequency range.

Via more aggressive modifications to conventional IC processes using MEMS technologies to both thicken metal turns (reducing series resistance) and suspend the inductor turns away from the substrate (reducing substrate losses), inductors with  $Q$ 's as high as 85 at 1 GHz have been demonstrated. Rows 3 and 4 of Table 4 present two such approaches: in row 3, one where planar spiral inductor turns are suspended high above the substrate, achieving a  $Q$  of 28 for 5 nH of inductance at 1.8 GHz [37][38]; and in row 4, one that utilizes planar processing together with self-assembling stresses to realize a solenoid inductor with axis parallel to substrate, and therefore magnetic field lines that run above and parallel to the substrate that generate much smaller eddy currents than planar spirals, allowing this inductor to achieve a  $Q$  of 85 for 7.5 nH at 1 GHz [11].

Although not the  $Q \sim 300$  needed for multi-band tunable RF filters, this  $Q \sim 85$ , when paired with a  $\mu$ mechanical capacitor, should allow the implementation of low noise VCO's with lower power consumption than those using conventional IC technology [40]. Tunable bias/matching networks that can reduce

power consumption in power amplifiers should also be feasible.

### 3.3 Micromechanical Switches

Micromechanical switches, such as depicted in row 5 of Table 4, often have a similar structure to the beam resonator of row 1 in Table 1, but are operated in a binary fashion: when the beam is up, the switch is open; when the beam is pulled down (e.g., by an electrostatic force), the switch is closed. Again, due to their metal construction made possible by MEMS technology,  $\mu$ mechanical switches post much smaller insertion losses than their FET-based counterparts (0.1 dB versus 2 dB) and are many times more linear, with  $IIP_3$ 's  $>66$  dBm. Although their switching times on the order of  $\mu$ s are much slower than that of FETs, they are still adequate for antenna switching, switchable filter, and phased array antenna applications, provided their high switching voltage levels can be reduced or accommodated. If achievable, the above applications are desirable for multi-band reconfigurability in handsets and for diversity against multi-path fading.

For some time now, the wireless industry has been awaiting improvements in the reliability of micromechanical switches. In particular, among the RF MEMS devices discussed in this paper, only RF switches require that actual contact between two micromechanical structures be made; the other devices only involve movements relative to a fixed electrode, without any contact. As a result, unlike the other RF MEMS devices, switches must overcome contact evolution, whereby changes to the beam-to-electrode contact interface incurred as the number of switching cycles rises eventually lead to switch failure. The mechanism for failure depends upon the type of switch. For direct contact switches operated under "cold-switched" conditions, where RF signals are not present when the switch makes an on/off (or off/on) transition, failure often results when either the contacts weld shut or the contact surfaces develop a dielectric film that prevents electrical contact. For capacitive switches, such as that in [12], for which a dielectric film prevents direct contact between beam and electrode, but an ac short ensues when the beam is brought into contact with the dielectric film, the failure mechanism is often related to charging of the dielectric material until a beam-to-electrode voltage is developed that either holds the switch down (i.e., failed shut), or that reduces the force of the applied actuation voltage to the point of preventing beam pull-down (i.e., failed open).

Given these failure mechanisms, contact interface or dielectric engineering are important considerations when long-lasting RF MEMS switches are desired. But environmental control is perhaps equally impor-

tant, since charging of dielectrics and growth of dielectrics are both functions of the humidity and gaseous environment surrounding the switch structure. In fact, it was the right combination of contact engineering and packaging that allowed the RF MEMS switch of row 5 in Table 4 (by Radant MEMS [39]) to achieve a lifetime greater than 600 billion cycles (and still counting) when cold-switched with 100mW RF power. This now more than satisfies the lifetime needs of commercial wireless applications, and the debut of RF MEMS switches into actual communication devices, if economically sensible, draws closer.

### 4.0 Conclusions

On-chip high- $Q$  passives attained via MEMS technologies have been described that can potentially play a key role in removing the board-level packaging requirements that currently constrain the size, power consumption, and robustness of communication transceivers. Indeed, the MEMS technologies used to implement vibrating on-chip resonators, tunable capacitors, isolated inductors, and low loss mechanical switches, might someday enable single-chip wireless devices that fully integrate these high- $Q$  passives together with IC transistors. By combining the strengths of integrated  $\mu$ mechanical and transistor circuits, using both in massive quantities, previously unachievable functions become possible that may soon enable alternative transceiver architectures with substantial performance gains.

**Acknowledgements.** Much of the work reported here was supported under the DARPA NMAPS Program and by the NSF ERC in WIMS.

### References.

- [1] A. A. Abidi, "Direct-conversion radio transceivers for digital comms," *IEEE J. Solid-State Circuits*, vol. 30, No. 12, pp. 1399-1410, Dec. 1995.
- [2] C.P. Yue and S.S. Wong, "On-chip spiral inductors with patterned ground shields for Si-based RF IC's," *IEEE J. Solid-State Circuits*, vol. 33, no. 5, pp.743-752, May 1998.
- [3] C. T.-C. Nguyen, "Vibrating RF MEMS overview: applications to wireless communications (invited)," *Proceedings*, Photonics West: MOEMS-MEMS 2005, San Jose, California, Jan. 22-27, 2005, Paper No. 5715-201.
- [4] C. T.-C. Nguyen, "MEMS for frequency control and timing (invited)," *Proceedings*, Joint IEEE Int. Frequency Control/Precision Time & Time Interval Symposium, Vancouver, Canada, Aug. 29-31, 2005, pp. 1-11.
- [5] C. T.-C. Nguyen, "Transceiver front-end architectures using vibrating micromechanical signal processors," chapter in *RF Technologies for Low Power Wireless Communications*, edited by G. I. Haddad, T. Itoh, and J. Harvey, pp. 411-461. New York: Wiley IEEE-Press, 2001.
- [6] J. Wang, J. E. Butler, T. Feygelson, and C. T.-C. Nguyen, "1.51-GHz polydiamond  $\mu$ mechanical disk resonator with impedance-mismatched isolating support," *Proceedings*, IEEE Int. MEMS Conf., Maastricht, The Netherlands, Jan. 25-29, 2004, pp. 641-644.
- [7] S.-S. Li, Y.-W. Lin, Y. Xie, Z. Ren, and Clark T.-C. Nguyen,



- "Micromechanical hollow-disk ring resonators," *Proceedings, 17th Int. IEEE MEMS Conf.*, Maastricht, Netherlands, Jan. 25-29, 2004, pp. 821-824.
- [8] J. Wang, Z. Ren, and C. T.-C. Nguyen, "1.156-GHz self-aligned vibrating micromechanical disk resonator," *IEEE Trans. Ultrason., Ferroelect., Freq. Contr.*, vol. 51, no. 12, pp. 1607-1628, Dec. 2004.
- [9] D. J. Young and B. E. Boser, "A micromachined variable capacitor for monolithic low-noise VCOs," *Technical Digest, 1996 Solid-State Sensor and Actuator Workshop*, Hilton Head Island, South Carolina, June 3-6, 1996, pp. 86-89.
- [10] J.-B. Yoon and C. T.-C. Nguyen, "A high- $Q$  tunable micromechanical capacitor with movable dielectric for RF applications," *Technical Digest, IEEE Int. Electron Devices Meeting*, San Francisco, California, Dec. 11-13, 2000, pp. 489-492.
- [11] C. L. Chua, D. K. Fork, K. V. Schuylenbergh, and J.-P. Lu, "Out-of-plane high- $Q$  inductors on low-resistance silicon," *IEEE/ASME J. Microelectromech. Syst.*, vol. 12, no. 6, pp. 989-995, Dec. 2003.
- [12] C. Goldsmith, J. Randall, S. Eshelman, T. H. Lin, D. Denniston, S. Chen and B. Norvell, "Characteristics of micromachined switches at microwave frequencies," *IEEE MTT-S Digest*, pp. 1141-1144, June, 1996.
- [13] S.-S. Li, Y.-W. Lin, Z. Ren, and C. T.-C. Nguyen, "Self-switching vibrating micromechanical filter bank," *Proceedings, IEEE Combined Int. Frequency Control/Precision Time & Time Interval Symposium.*, Vancouver, Canada, Aug. 29-31, 2005, pp. 135-141.
- [14] C. T.-C. Nguyen and R. T. Howe, "An integrated CMOS micromechanical resonator high- $Q$  oscillator," *IEEE J. Solid-State Circuits*, vol. 34, no. 4, pp. 440-455, April 1999.
- [15] T. A. Core, W. K. Tsang, and S. J. Sherman, "Fabrication technology for an integrated surface-micromachined sensor," *Solid State Technology*, pp. 39-47, Oct. 1993.
- [16] A. E. Franke, J. M. Heck, T.-J. King and R. T. Howe, "Polycrystalline silicon-germanium films for integrated microsystems," *IEEE/ASME J. Microelectromech. Syst.*, vol. 12, no. 2, pp. 160-171, April 2003.
- [17] J. Gaspar, V. Chu, and J. P. Conde, "High- $Q$  thin-film silicon resonators processed at temperatures below 110°C on glass and plastic substrates," *Proceedings, 17th Int. IEEE MEMS Conf.*, Maastricht, The Netherlands, Jan. 25-29, 2004, pp. 633-636.
- [18] A.-C. Wong and C. T.-C. Nguyen, "Micromechanical mixer-filters ("mixlers")," *IEEE/ASME J. Microelectromech. Syst.*, vol. 13, no. 1, pp. 100-112, Feb. 2004.
- [19] W. -T. Hsu and C. T. -C. Nguyen, "Stiffness-compensated temperature-insensitive micromechanical resonators," *Tech. Digest, 2002 IEEE Int. MEMS Conf.*, Las Vegas, Nevada, Jan. 20-24, 2002, pp. 731-734.
- [20] F. D. Bannon III, J. R. Clark, and C. T.-C. Nguyen, "High frequency micromechanical filters," *IEEE J. Solid-State Circuits*, vol. 35, no. 4, pp. 512-526, April 2000.
- [21] K. Wang, A.-C. Wong, and C. T.-C. Nguyen, "VHF free-free beam high- $Q$  micromechanical resonators," *IEEE/ASME J. Microelectromech. Syst.*, vol. 9, no. 3, pp. 347-360, Sept. 2000.
- [22] M. A. Abdelmoneum, M. U. Demirci, and C. T.-C. Nguyen, "Stemless wine-glass-mode disk micromechanical resonators," *Proceedings, 16th Int. IEEE MEMS Conf.*, Kyoto, Japan, Jan. 19-23, 2003, pp. 698-701.
- [23] M. L. Roukes, "Nanoelectromechanical systems," *Tech. Dig., 2000 Solid-State Sensor and Actuator Workshop*, Hilton Head, South Carolina, June 4-8, 2000, pp. 367-376.
- [24] J. R. Vig and Y. Kim, "Noise in microelectromechanical system resonators," *IEEE Trans. Ultrason. Ferroelec. Freq. Contr.*, vol. 46, no. 6, pp. 1558-1565, Nov. 1999.
- [25] S. Pourkamali, *et al.*, "Vertical capacitive SiBARs," *Tech. Dig., 18<sup>th</sup> IEEE Int. Conf. on MEMS*, Miami Beach, Florida, Jan. 30-Feb. 3, 2005, pp. 211-214.
- [26] G. Piazza, *et al.*, "Low motional resistance ring-shaped contour-mode aluminum nitride piezoelectric  $\mu$ mechanical resonators for UHF applications," *Tech. Dig., 18<sup>th</sup> IEEE MEMS Conf.*, Miami Beach, FL, Jan. 30-Feb. 3, 2005, pp.20-23.
- [27] V. Kaajakari, J. Kiihamäki, A. Oja, H. Seppä, S. Pietikäinen, V. Kokkala, and H. Kuisma, "Stability of wafer level vacuum encapsulated single-crystal silicon resonators," *Digest of Technical Papers, Transducers'05*, Seoul, Korea, June 2005, pp. 916-919.
- [28] B. Kim, R. N. Candler, M. Hopcroft, M. Agarwal, W.-T. Park, and T. W. Kenny, "Frequency stability of wafer-scale encapsulated MEMS resonators," *Digest of Technical Papers, Int. Conf. on Solid-State Sensors, Actuators, and Microsystems (Transducers'05)*, Seoul, Korea, June 2005, pp. 1965-1968.
- [29] Y.-W. Lin, S.-S. Li, Z. Ren, and C. T.-C. Nguyen, "Vibrating micromechanical resonators with solid dielectric capacitive-transducer 'gaps'," *Proceedings, IEEE Combined Int. Frequency Control/Precision Time & Time Interval Symposium.*, Vancouver, Canada, Aug. 29-31, 2005, pp. 128-134.
- [30] D. T. Chang, *et al.*, "A new MEMS-based quartz resonator technology," *Tech. Dig., Solid-State Sensor, Actuator, and Microsystems Workshop*, Hilton Head, SC, June 6-10, pp. 41-44.
- [31] K. Wang and C. T.-C. Nguyen, "High-order medium frequency micromechanical electronic filters," *IEEE/ASME J. Microelectromech. Syst.*, vol. 8, no. 4, pp. 534-557, Dec. 1999.
- [32] S.-S. Li, *et al.*, "Bridged  $\mu$ mechanical filters," *Proceedings, IEEE Int. Ultrasonics, Ferroelects., and Freq. Cont. 50th Anniv. Joint Conf.*, Montreal, Canada, Aug. 24-27, 2004, pp. 144-150.
- [33] M. U. Demirci, *et al.*, "Mech. corner-coupled square microresonator array for reduced series motional resistance," *Dig. of Tech. Papers, Transducers'03*, Boston, MA, June 8-12, 2003, pp. 955-958.
- [34] M. U. Demirci and C. T.-C. Nguyen, "A low impedance VHF micromechanical filter using coupled-array composite resonators," *Dig. of Tech. Papers, Transducers'05*, Seoul, Korea, June 5-9, 2005.
- [35] R. Navid, J. R. Clark, M. Demirci, and C. T.-C. Nguyen, "Third-order intermodulation distortion in capacitively-driven CC-beam micromechanical resonators," *Tech. Digest, 14<sup>th</sup> Int. IEEE MEMS Conf.*, Interlaken, Switzerland, Jan. 21-25, 2001, pp. 228-231.
- [36] Y.-W. Lin, S.-S. Li, Z. Ren, and C. T.-C. Nguyen, "Third-order intermodulation distortion in capacitively-driven VHF micromechanical resonators," *Proceedings, IEEE Ultrasonics Symposium*, Sept. 18-21, 2005, to be published.
- [37] J.-B. Yoon, C.-H. Han, E. Yoon, and C.-K. Kim, "Monolithic high- $Q$  overhang inductors fabricated on silicon and glass substrates," *IEEE Int. Electron Devices Mtg. (IEDM)*, Dec. 5-8, 1999, pp. 753-756.
- [38] J.-B. Yoon, Y.-S. Choi, B.-I. Kim, Y. Eo, and E. Yoon, "CMOS-compatible surface-micromachined suspended-spiral inductors for multi-GHz silicon RF IC's," *IEEE Electron Device Lett.*, vol. 23, no. 10, pp. 591-593, Oct. 2002.
- [39] J. Maciel, S. Majumder, R. Morrison, and J. Lampen, "Reliability testing of ohmic MEMS switches," in *IEEE MTT-S 2004 Int. Microwave Symp. Dig.*, Fort Worth, TX, Workshop WFF.1.
- [40] P. Q. Chen and Y.-J. Chan, "Improved microwave performance on low-resistivity Si substrates by Si<sup>+</sup> ion impalnation," *IEEE Trans. Microwave Theory Tech.*, vol. 48, no. 9, pp. 1582-1585, Sept. 2000.
- [41] A. Dec and K. Suyama, "A 1.9-GHz CMOS VCO with micromachined electromechanically tunable capacitors," *IEEE J. Solid-State Circuits*, vol. 35, no. 8, pp. 1231-1237, Aug. 2000.